Plane Strain Finite Element Modeling for Interface Debonding in AA1100/Silicon Oxide Nanoparticulate Metal Matrix Composites

[1]P. M. Jebaraj and A. Chennakesava Reddy[2]

[1]Professor, Department of Mechanical Engineering, Dr. Ambdekar Institute of Technology, Bangalore, India
[2]Assistant Professor, Department of Mechanical Engineering, MJ College of Engineering and Technology, Hyderabad, India
dr_acreddy@yahoo.com

Abstract: *Square array unit cell/2-D elliptical particulate RVE models were used to evaluate interface debonding using two-dimensional finite element methods under plane strain conditions. The particulate metal matrix composites are silicon oxide/AA1100 alloy at different volume fractions of silicon oxide. There is strong probability of interface debonding at all volume fractions of silicon oxide.*

Keywords: AA1100*, silicon oxide, elliptical particle, RVE model, finite element analysis, debonding.*

1. INTRODUCTION

Metal matrix composites have experienced an exceptional development over the last decade, mainly in the field of aerospace applications. Very tough interfaces result in negligible debonding and in very low energy absorption in the axial fracture of the composite, while excessive debonding beyond the natural necking length adversely affects the transverse strength of the composite. The actual development of debonding in response to a deformation-governed mix of modes of interface fracture is the subject of the micromechanical model. The interface debonding was carried out in the metal matrix composites comprising of a variety combinations of matrix alloy and particulates [1-10].

The purpose of this paper is to evaluate debonding in AA1100 alloy/silicon oxide particulate metal matrix composites. Representative volume elements (RVEs) models were modeled using finite element method. The RVEs were taken from the periodic 2-D elliptical particulates in a square array distribution.

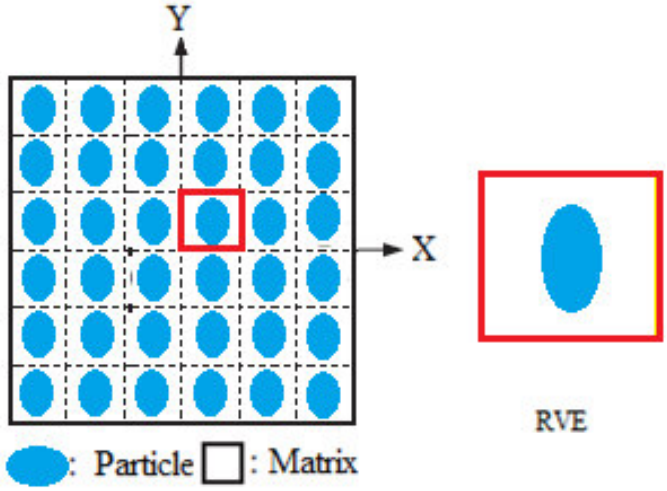

Figure 1: The RVE model: (a) particle distribution and (b) RVE scheme.

2. MATERIALS AND METHODS

The AA1100 alloy/silicon oxide nanoparticulate metal matrix composites were used in the present work with 10%, 20%, and 30% volume fractions of silicon oxide. The periodic model for the representative volume element (RVE) scheme as shown in figure 1 was used to analyze the composites with ANSYS software code. The RVE scheme was constructed from 2-D elliptical particulates in a square array particulate distribution. The perfect adhesion was assumed between silicon nitride particle and AA8090 alloy matrix. PLANE183 element was used for the matrix and the nanoparticle. The interface between particle and matrix was modeled using CONTACT -172 elements.

If particle fracture occurs when the stress in the particle reaches its ultimate tensile strength, $\sigma_{p,uts}$, then setting the boundary condition at

$$\sigma_p = \sigma_{p,\,uts} \quad (1)$$

and substituting into Eq.(1) gives a relationship between the strength of the particle and the interfacial shear stress such that if

$$\sigma_{P,uts} < \frac{2\tau}{n} \quad (2)$$

Then the particle will fracture. Similarly if interfacial debonding/yielding is considered to occur when the interfacial shear stress reaches its shear strength

$$\tau = \tau_{max} \quad (3)$$

Then by substituting Eq. (5) into Eq.(1) a boundary condition for particle/matrix interfacial fracture can be established whereby,

$$\tau_{max} < \frac{n\sigma_p}{2} \quad (4)$$

This approach suggests that the outcome of a matrix crack impinging on an embedded particle depends on the balance between the particle strength and the shear strength of the interface.

A linear stress–strain relation at the macro level can be formulated as follows:

$$\bar{\sigma} = \overline{C}\,\bar{\varepsilon} \quad (5)$$

where $\bar{\sigma}$ is macro stress, and $\bar{\varepsilon}$ represents macro total strain and $\overline{C}$ and is macro stiffness matrix.

For plane strain conditions, the macro stress- macro strain relation is as follows:

$$\begin{Bmatrix} \overline{\sigma_x} \\ \overline{\sigma_y} \\ \overline{\tau_{xy}} \end{Bmatrix} = \begin{bmatrix} \overline{C_{11}} & \overline{C_{12}} & 0 \\ \overline{C_{21}} & \overline{C_{22}} & 0 \\ 0 & 0 & \overline{C_{33}} \end{bmatrix} \times \begin{Bmatrix} \overline{\varepsilon_x} \\ \overline{\varepsilon_y} \\ \overline{\gamma_{xy}} \end{Bmatrix} \quad (6)$$

The interfacial tractions can be obtained by transforming the micro stresses at the interface as given in Eq. (3):

$$t = \begin{Bmatrix} t_z \\ t_n \\ t_t \end{Bmatrix} = T\sigma \quad (7)$$

where, $T = \begin{bmatrix} 0 & 0 & 0 \\ cos^2\theta & sin^2\theta & 2sin\theta cos\theta \\ -sin\theta cos\theta & sin\theta cos\theta & cos^2\theta - sin^2\theta \end{bmatrix}$

3. RESULTS AND DISCUSSION

The effect of volume fraction of silicon nitride on the elastic moduli, E_x, E_y and G_{xy} is shown figure 2a. The tensile elastic modulus, compressive modulus and shear modulus were nearly independent of silicon oxide content in the composites. The major Poisson's ratio decreased with increase of volume fraction of silicon oxide (figure 2b).

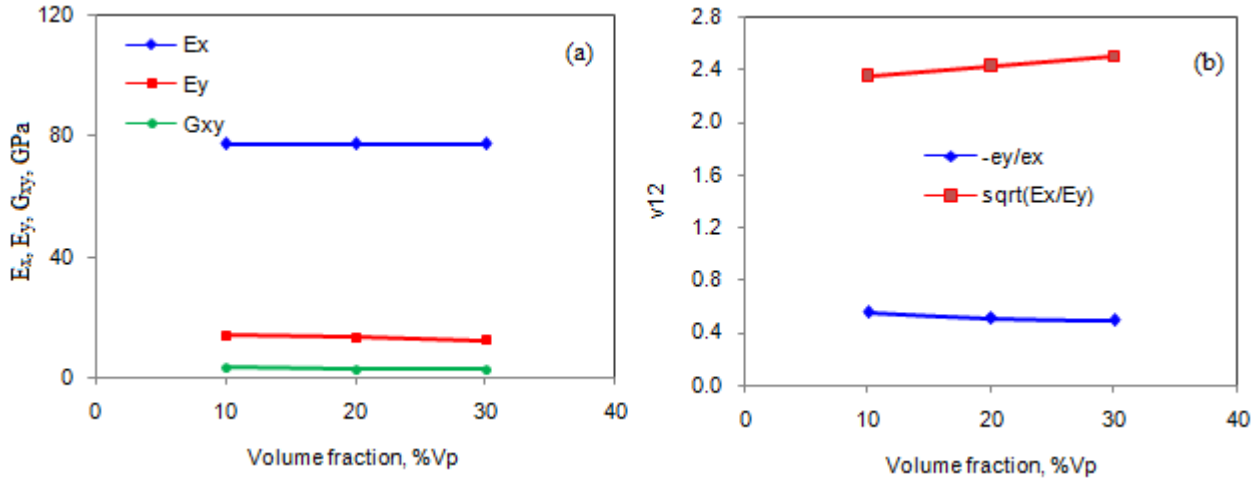

Figure 2: Effect of volume fraction on effective material properties.

The debonding was occurred in all the AA1100/SiO_2 nanoparticulate composites as shown in figure 3b. The condition, $\tau_{max} < n\sigma_p/2$ was satisfied for the occurrence of debonding in all the composites. The shear stress developed at the interface increased with the increase of silicon oxide content in the composites. The reasons for the interface debonding were of normal traction developed at the interface (figure 4). The debonding phenomenon is clearly observed in the composite having 30% silicon nitride (figure 5). The silicon nitride particulate fracture was not noticed as the condition $\sigma_p \leq 2\tau/n$ is not satisfied as shown in figure 3a. The strength of silicon nitride is higher than the shear stress required for fracturing silicon nitride particulates. The von Mises stresses increased with the increase of silicon oxide content in the composites.

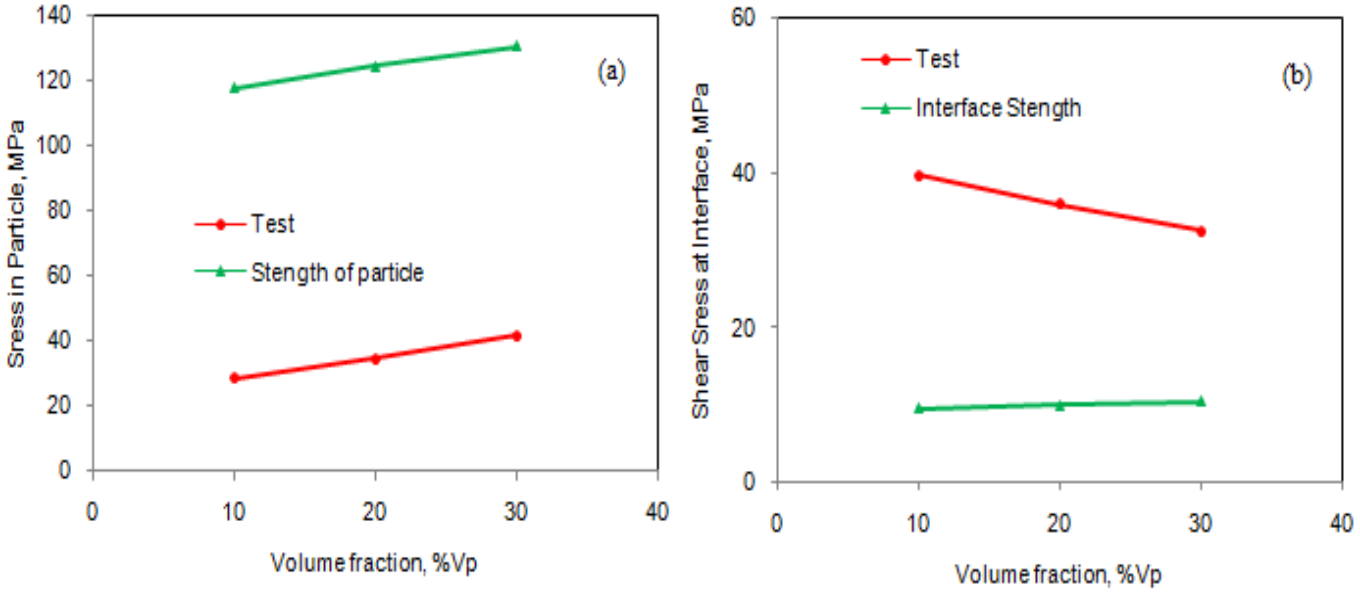

Figure 3: Fracture criteria of: (a) particulate fracture and (b) interface debonding.

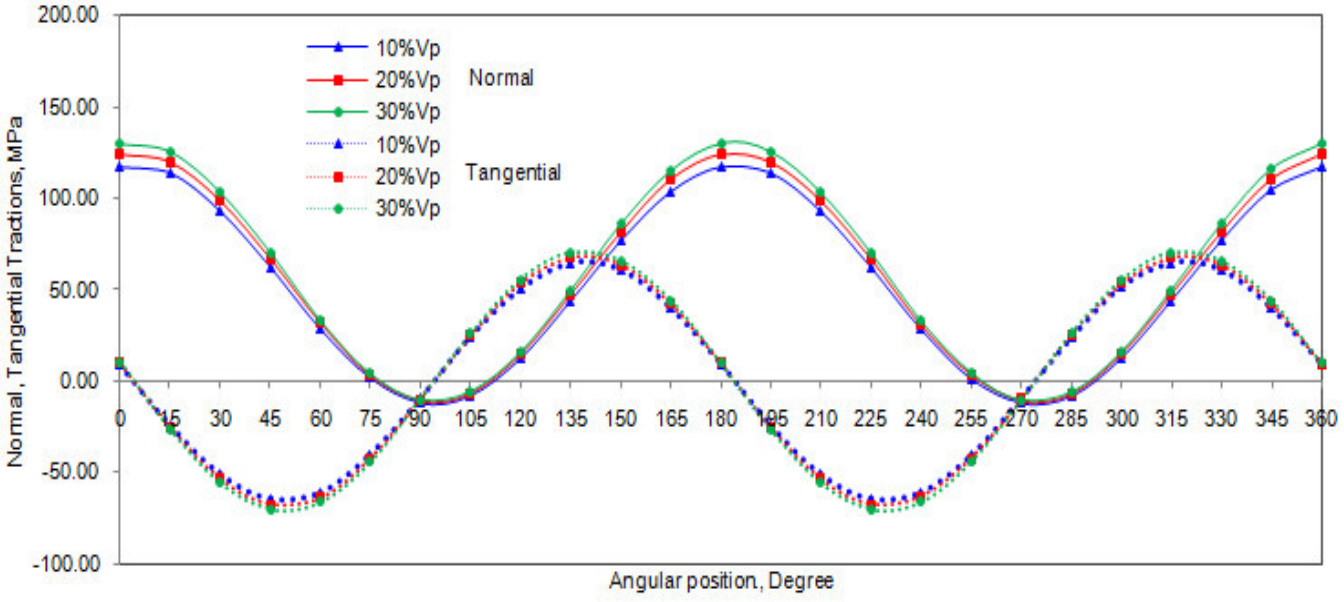

Figure 4: Normal and tangential interactions.

4. CONCLUSION

The interface debonding took place at all volume fractions of SiO_2 in the composite. The normal tractions along the interface promote interfacial debonding.

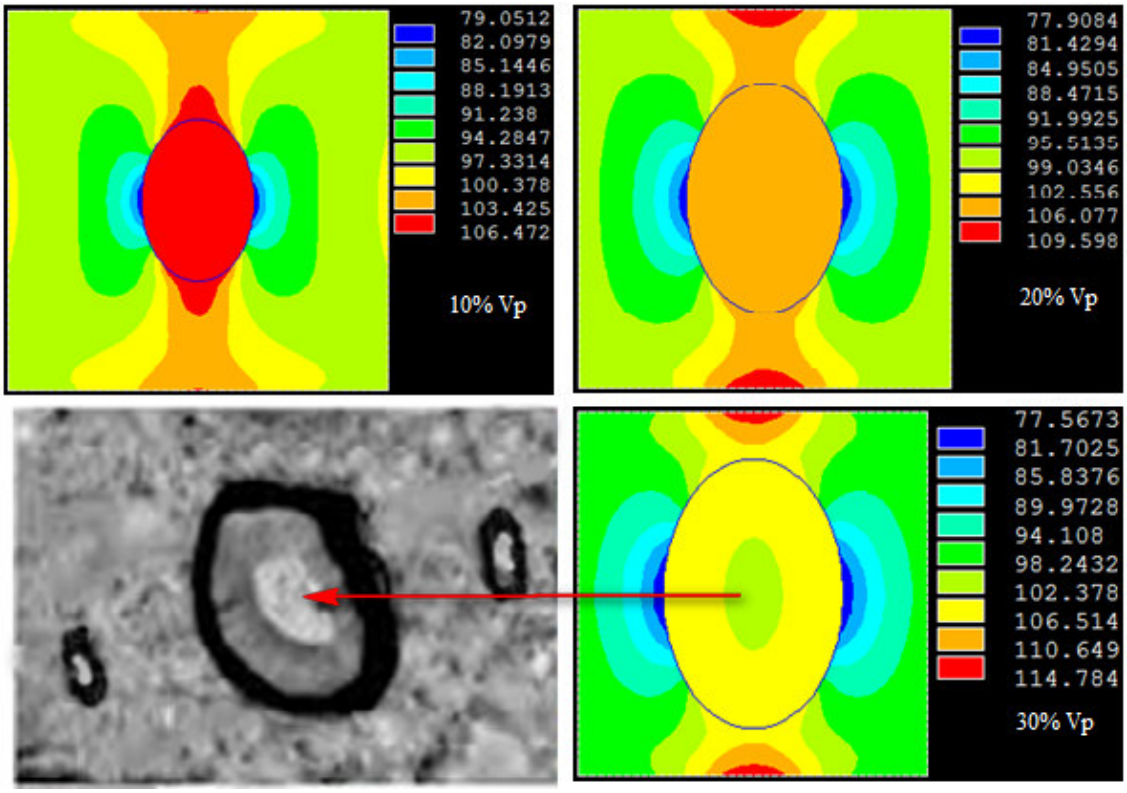

Figure 5: Results obtained from finite element analysis: von Mises stresses.

REFERENCES

1. S. Sundara Rajan and A. Chennakesava Reddy, Assessment of Tensile Behavior of Boron Carbide/AA2024 Alloy Metal Matrix Composites, 1st International Conference on Composite Materials and Characterization, Bangalore, March 1997, pp.160-163.
2. P. Martin Jebaraj and A. Chennakesava Reddy, Prediction of Micro-stresses and interfacial Tractions in Boron Carbide/AA6061 Alloy Metal Matrix Composites, 1st International Conference on Composite Materials and Characterization, Bangalore, March 1997, pp. 183-185.
3. B. Kotiveera Chari and A. Chennakesava Reddy, Computation of Micro-stresses and interfacial Tractions in Boron Carbide/AA7020 Alloy Metal Matrix Composites, 1st International Conference on Composite Materials and Characterization, Bangalore, March 1997, pp. 186-188.
4. P. Martin Jebaraj, A. Chennakesava Reddy, Effect of Interfacial Debonding on Stiffness of Titanium Boride/AA5050 Alloy Metal Matrix Composites, 1st National Conference on Modern Materials and Manufacturing , Pune, 19-20 December, 1997.
5. S. Sundara Rajan, A. Chennakesava Reddy, Micromechanical modeling of Titanium Boride/AA7020 Alloy Metal Matrix Composites in Finite Element Analysis using RVE Model, 1st National Conference on Modern Materials and Manufacturing , Pune, 19-20 December, 1997.
6. P. Martin Jebaraj, A. Chennakesava Reddy, Effect of Interfacial Tractions of Rectangular Titanium Boride Particulate/AA8090 Alloy Metal Matrix Composites , 1st National Conference on Modern Materials and Manufacturing , Pune, 19-20 December, 1997.
7. S. Sundara Rajan, A. Chennakesava Reddy, Cohesive Zone interfacial debonding of Silicon Nitride/AA1100 Alloy Metal Matrix Composites Using Finite Element Analysis , 1st National Conference on Modern Materials and Manufacturing , Pune, 19-20 December, 1997.
8. S. Sundara Rajan, A. Chennakesava Reddy, Simulation of Micromechanics for interfacial debonding in Silicon Nitride/AA2024 Alloy Metal Matrix Composites , 1st National Conference on Modern Materials and Manufacturing , Pune, 19-20 December, 1997.
9. P. Martin Jebaraj, A. Chennakesava Reddy, Finite Element Analysis for Assessment of Dislocation and Debonding Events in Silicon Nitride/AA3003 Alloy Metal Matrix Composites, 1st National Conference on Modern Materials and Manufacturing , Pune, 19-20 December, 1997.
10. A. Chennakesava Reddy, Evaluation of Debonding and Dislocation Occurrences in Rhombus Silicon Nitride Particulate/AA4015 Alloy Metal Matrix Composites, 1st National Conference on Modern Materials and Manufacturing, Pune, India, 19-20 December, 278-282, 1997.